

TABLE OF CONTENTS

	Page
Acknowledgements	iii
Abstract-English	v
Abstract-Thai	viii
List of tables	xvii
List of figures	xix
Abbreviations and symbols	xxv
Chapter 1 Introduction	1
1.1 Foreword	1
1.2 Objectives of the thesis	5
1.3 Outline of the thesis	7
Chapter 2 Literature review and theoretical background	10
2.1 Background on polymer science	10
2.1.1 Polymer crystallinity	10
2.1.2 Comparison of semicrystalline and amorphous polymers	15
2.1.3 Crystallinity determination	17
2.1.4 Thermal properties of polymers	19
2.1.4.1 Glass transition temperature	19
2.1.4.2 Crystalline transition (melting) temperature	20
2.1.5 Thermal analytical techniques	21
2.1.6 Mechanical properties of polymers	23

	Page
2.1.6.1 Tensile properties	27
2.1.6.2 Impact properties	31
2.1.7 Swelling of polymer in a solvent	33
2.2 Background on plastic foams	40
2.2.1 Introduction of plastic foams	40
2.2.2 Composition of plastic foams	42
2.2.2.1 Plastic matrix	42
2.2.2.2 Gas phase and blowing agents	42
2.2.2.3 Nucleating agents (nucleants)	46
2.2.2.4 Stabilizers	47
2.2.2.5 Cell structure	48
2.2.3 Classification of foams	49
2.2.3.1 High-density foams	49
2.2.3.2 Low-density foams	49
2.2.4 Foaming methods and the production	52
2.2.4.1 Production of high-density foams	54
2.2.4.2 Production of low-density foams	54
2.2.5 Conceptual design and detail of batch foaming process equipment	55
2.2.6 Conceptual design and detail of tandem extrusion system (Continuous foaming process)	58
2.2.6.1 Detail Design of the Tandem Extrusion Line	62

	Page
2.3 Theoretical background	70
2.3.1 Foam formation	70
2.3.1.1 Polymer/gas formation	71
2.3.1.2 Cell nucleation	71
2.3.1.3 Cell growth	75
2.3.1.4 Foam stability	77
2.3.2 Solubility and diffusivity	78
2.3.2.1 Solubility	78
2.3.2.2 Diffusivity	82
2.3.3 Selection of blowing agent	83
2.4 Microcellular foams and the production strategies	85
2.4.1 Batch microcellular processing	88
2.4.2 Semi-continuous microcellular processing	91
2.4.3 Continuous microcellular processing	92
2.5 Low-density, fine-celled foams and the production strategies	94
2.5.1 Fundamental mechanisms governing volume expansion of PP foams	95
2.5.2 Strategies for promoting high volume expansion	99
2.6 Characterization of final foams	101
Chapter 3 Solid-state batch foaming process for microcellular PP foam manufacturing	104
3.1 Introduction	104
3.2 Research objectives	107

	Page
3.3 Experimental	108
3.3.1 Materials	108
3.3.2 Sample preparation	109
3.3.3 Determination of a solvent for using in the swelling step	110
3.3.4 Investigation of chloroform performance on crystallinity of PP	111
3.3.5 Saturation time of CO ₂ in PP determination	113
3.3.6 Foaming procedure	114
3.3.7 Investigation of foam Characteristics	115
3.3.8 Mechanical properties testing	116
3.3.8.1 Tensile testing	116
3.3.8.2 Impact testing	117
3.4 Results and discussions	118
3.4.1 Properties of PP pellets	118
3.4.2 Solvent swelling behaviors of PP samples	118
3.4.3 Effect of chloroform on thermal property and crystallinity of PP	119
3.4.4 Saturated time for CO ₂ absorption in PP	120
3.4.5 Effects of chloroform and processing condition on density and void fraction	120
3.4.6 Effects of chloroform and processing condition on cell morphology	123

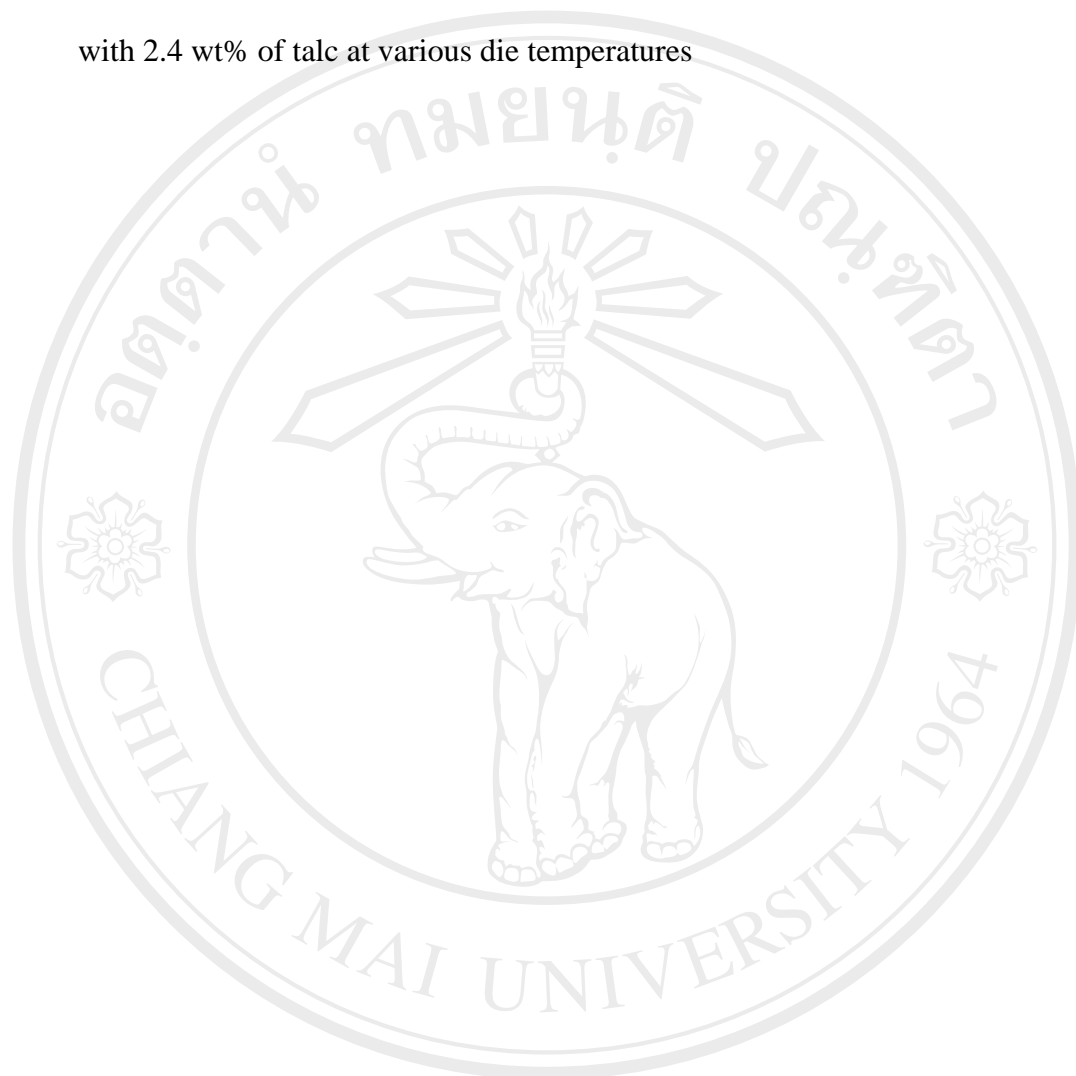
	Page
3.4.7 Effects of foaming conditions on the mechanical properties	132
3.4.7.1 Tensile properties of PP foams	132
3.4.7.2 Impact strength	143
3.5 Conclusions	147
Chapter 4 Continuous foaming process for low density and Fine-celled PP foam manufacturing	150
4.1 Introduction	150
4.2 Manufacturing of low-density and fine-celled PP foams	160
4.3 Research objective	164
4.4 Experimental	165
4.4.1 Materials	165
4.4.2 Investigation of polypropylene (Honam SMS-514) properties	165
4.4.3 Foaming procedure	167
4.4.4 Sample characterization	169
4.5 Results and discussion	170
4.5.1 Properties of PP pellets (Honam SMS-514)	170
4.5.2 Pressure-temperature profile of foaming process	171
4.5.3 Densities of PP foams	172
4.5.4 Effects of processing parameters on the volume expansion ratio	175

	Page
4.5.5 Effects of processing parameters on cell nucleation	184
4.6 Conclusions	192
Chapter 5 Summary and conclusions	194
Chapter 6 Recommendations and future work	199
6.1 Solid-state batch foaming process	199
6.2 Continuous foaming process	202
References	205
Appendix	218
Curriculum vitae	243

LIST OF TABLES

Table	Page
2.1 Comparison of semicrystalline and amorphous polymers	16
2.2 Typical market for high-density thermoplastic foams	50
2.3 Typical markets for low-density foams	51
2.4 Solubility of carbon dioxide and nitrogen in PP at 433.2 K and 473.2 K	81
2.5 Relative diffusion rates of blowing gases through PE and PP at 188 °C (relative to nitrogen in PE, 6.04×10^{-5} cm ² /s)	83
3.1 The properties of PP pellets	108
3.2 Thermal properties and % crystallinity of non-solvent and chloroform-swollen samples	112
4.1 Calculated geometry, residence time, and pressure drop rate of the dies for HMS PP	154
4.2 Re-calibrated geometries of the dies for HMS PP	155
4.3 Melt flow index of Honam SMS-514 at 230 °C and 2.16 kg	166
4.4 Density of PP pellets at 22 °C	172
4.5 The average density of PP foams with 1, 3, and 5 wt% of CO ₂ without talc at various die temperatures	173
4.6 The average density of PP foams with 1, 3, and 5 wt% of CO ₂ with 0.8 wt% of talc at various die temperatures	173
4.7 The average density of PP foams with 1, 3, and 5 wt% of CO ₂ with 1.6 wt% of talc at various die temperatures	174

Table	Page
4.8 The average density of PP foams with 1, 3, and 5 wt% of CO ₂ with 2.4 wt% of talc at various die temperatures	174



ลิขสิทธิ์มหาวิทยาลัยเชียงใหม่
Copyright© by Chiang Mai University
All rights reserved

LIST OF FIGURES

Figure	Page
2.1 Crosslinking process	10
2.2 Structure of long plastic molecules	13
2.3 Schematic of differential scanning calorimeter (DSC)	23
2.4 Typical DSC thermogram of completely amorphous polymer	23
2.5 A typical stress-strain diagram	25
2.6 Typical tensile stress-strain curves for general polymers	26
2.7 Typical test setup and specimen	27
2.8 Impact test setups	32
2.9 The Lattices model of solubility of (a) small molecules (●) and (b) large polymeric molecules (●—●)	34
2.10 Models of slabs of typical closed-cell foams and open-cell foams	41
2.11 Phase diagram of supercritical carbon dioxide	45
2.12 A gas pressure chamber of the gas saturation step	57
2.13 Experimental setup of solid-state foaming process	58
2.14 Schematic of the tandem extrusion system	63
2.15 Schematic of the extruder mixing section	64
2.16 Schematic of the gear pump	66
2.17 Schematic of the heat exchanger (courtesy of Behraves)	68
2.18 A schematic of the filament die	69
2.19 A schematic of the cooling sleeve to be mounted on the nucleation nozzle	70

Figure	Page
2.20 Sorption isotherm for typical polymer/gas system	79
2.21 Solubility of carbon dioxide and nitrogen in PP	80
2.22 Batch microcellular foaming process	90
2.23 Semi-continuous microcellular foaming process	92
2.24 Schematic of continuous microcellular foaming process	94
2.25 Shapes of extrudate PP foams at various temperatures at the die	96
2.26 Schematic of volume expansion mechanism	97
3.1 DSC thermogram of PP pellets (EP380T SW-844) in the range of 25-200 °C at heating rate of 10 °C/min analyzed by DSC7, Perkin-Elmer	109
3.2 Swelling behaviors of PP sheet (0.5 mm) with various solvents at ambient condition	111
3.3 DSC thermograms of (a) Chloroform-swollen sample and (b) Non-solvent sample at 25-200 °C and the heating rate of 10 °C/min under N ₂ atmosphere	112
3.4 Gas absorption curve of CO ₂ in PP sheet with 0.5 mm of thickness at 5.5 MPa and 25 °C ± 2 °C	114
3.5 Experimental setup for solid-state batch foaming process	115
3.6 Void fraction of PP foams with various thicknesses at various processing conditions; (a) Non-solvent foams and (b) Chloroform-swollen foams	123
3.7 SEM images of PP foams (0.5 mm) at 1000 times of magnification	125

Figure	Page
3.8 Cell densities (cells/cm ³) of PP foams with various thicknesses at various processing conditions; (a) Non-solvent foams and (b) Chloroform-swollen foams	126
3.9 Average Cell size (μm) of PP foams with various thicknesses at various processing conditions; (a) Non-solvent foams and (b) Chloroform-swollen foams	127
3.10 SEM images of (a)-(c) non-solvent foams and (d)-(f) chloroform-swollen foams at 50 °C, 1000 times of magnification	128
3.11 SEM images of (a) non-solvent foams and (b) chloroform-swollen foams at 155 °C (1.0 mm in thickness), 1000 times of magnification	130
3.12 SEM images of PP foams with 1.5 mm of thickness at 1000 times of magnification	131
3.13 Stress-strain curves of all samples with 0.5 mm of thickness at various foaming conditions (a) non-solvent foams and (b) chloroform-swollen foams	134
3.14 Stress-strain curves of all samples with 1.0 mm of thickness at various foaming conditions (a) non-solvent foams and (b) chloroform-swollen foams	135
3.15 Stress-strain curves of all samples with 1.5 mm of thickness at various foaming conditions (a) non-solvent foams and (b) chloroform-swollen foams	136

Figure	Page
3.16 Tensile strength at maximum load of all samples at various foaming temperatures; (a) Un-foamed sheets (b) PP foams with 0.5 mm (c) PP foams with 1.0 mm, and (d) PP foams with 1.5 mm	138
3.17 Elongation at maximum load of all samples at various foaming temperatures; (a) Un-foamed sheets (b) PP foams with 0.5 mm (c) PP foams with 1.0 mm, and (d) PP foams with 1.5 mm	140
3.18 Young's modulus of all samples at various foaming temperatures; (a) Un-foamed sheets (b) PP foams with 0.5 mm (c) PP foams with 1.0 mm, and (d) PP foams with 1.5 mm	143
3.19 Specific impact strength of all samples at various temperatures	146
3.20 Fractography of the samples after impact testing; (a) un-foamed sample, (b) non-solvent and (c) chloroform-swollen PP foams at 165 °C	146
3.21 Macroscopic (SEM images) of PP foams at 165 °C after impact testing; (a) non-solvent foam and (c) chloroform-swollen foam	147
4.1 Targeted pressure drop and pressure drop rate for the 8 filamentary dies for HMS PP	153
4.2 Expansion ratios versus die pressure at; (a) 1 wt% of CO ₂ , (b) 3 wt% of CO ₂ , and (c) 5 wt% of CO ₂ , respectively	156
4.3 Cell densities versus die pressures at; (a) 1 wt% of CO ₂ , (b) 3 wt% of CO ₂ , and (c) 5 wt% of CO ₂ , respectively	157
4.4 DSC thermogram of HMS-branched PP resin at the heating and cooling rate of 10 °C/min	166

Figure	Page
4.5 Pressure-temperature profile of foaming process of Honam SMS-514 with various processing conditions	172
4.6 Volume expansion ratios of PP foams with 1, 3, and 5 wt% of CO ₂ without talc at various die temperatures	176
4.7 Volume expansion ratios of PP foams with 1, 3, and 5 wt% of CO ₂ with 0.8 wt% of talc at various die temperatures	177
4.8 Volume expansion ratios of PP foams with 1, 3, and 5 wt% of CO ₂ with 1.6 wt% of talc at various die temperatures	177
4.9 Volume expansion ratios of PP foams with 1, 3, and 5 wt% of CO ₂ with 2.4 wt% of talc at various die temperatures	178
4.10 Maximum volume expansion ratios of PP foams versus CO ₂ content	180
4.11 Maximum volume expansion ratios of PP foams versus talc content	180
4.12 Blowing agent efficiency of PP foams with 1, 3, and 5 wt% of CO ₂ without talc at various die temperatures	181
4.13 Blowing agent efficiency of PP foams with 1, 3, and 5 wt% of CO ₂ with 0.8 wt% of talc at various die temperatures	182
4.14 Blowing agent efficiency of PP foams with 1, 3, and 5 wt% of CO ₂ with 1.6 wt% of talc at various die temperatures	182
4.15 Blowing agent efficiency of PP foams with 1, 3, and 5 wt% of CO ₂ with 2.4 wt% of talc at various die temperatures	183
4.16 SEM images (at 200 times of magnification) of PP foams with 0.8 wt% of talc and 5 wt% of CO ₂ at various die temperatures	184

Figure	Page
4.17 Cell densities of PP foams with 1, 3, and 5 wt% of CO ₂ and without talc at various die temperatures	185
4.18 Cell densities of PP foams with 1, 3, and 5 wt% of CO ₂ with 0.8 wt% of talc at various die temperatures	186
4.19 Cell densities of PP foams with 1, 3, and 5 wt% of CO ₂ with 1.6 wt% of talc at various die temperatures	186
4.20 Cell densities of PP foams with 1, 3, and 5 wt% of CO ₂ with 2.4 wt% of talc at various die temperatures	187
4.21 Maximum cell densities of PP foams versus CO ₂ content	188
4.22 Maximum cell densities of PP foams versus talc content	189
4.23 Average cell size of PP foams with 1, 3, and 5 wt% of CO ₂ without talc at various die temperatures	190
4.24 Average cell size of PP foams with 1, 3, and 5 wt% of CO ₂ with 0.8 wt% of talc content at various die temperatures	191
4.25 Average cell size of PP foams with 1, 3, and 5 wt% of CO ₂ with 1.6 wt% of talc content at various die temperatures	191
4.26 Average cell size of PP foams with 1, 3, and 5 wt% of CO ₂ with 2.4 wt% of talc content at various die temperatures	192
6.1 Expansion step and the final foamed PP sheet	201

ABBREVIATIONS AND SYMBOLS

a	Consistency parameter in power law ($\text{Pa}\cdot\text{s}^n$)
A	Matrix representing the complete relationship between FR_s and DP_s
A_i	Defined area of the SEM image
C	Constant that equals to 1.0 when the property is modulus and equals to 0.3 when it is the collapse stress
C_0 and C_1	Concentrations of homogeneous nucleation sites and heterogeneous nucleation sites, respectively
C_s	Solubility of gas in the polymer (cm^3/g) or ($\text{g}_{\text{gas}}/\text{g}_{\text{polymer}}$)
d	Average cell size
dp/dt	Pressure drop rate (Pa/s)
D	Diffusion coefficient or diffusivity (cm^2/s)
D_0	Material dependent diffusion coefficient
DP_s	Design parameters
E_D	Activation energy in diffusion
f_0 and f_1	Frequency factors of gas molecules joining the nucleus ($1/\text{s}$) for homogeneous nucleation and heterogeneous nucleation, respectively
FR_s	Functional requirements
H	Henry's law constant (cm^3 [STP]/ $\text{g}\cdot\text{Pa}$)
H_0	Solubility coefficient constant (cm^3 [STP]/ $\text{g}\cdot\text{Pa}$)

HMS	High-melt-strength
k	Boltzman's constant (J/K)
l	Diffusion distance
L^2	Defined area ($L \times L$) of the SEM image
L_{die}	length of the nozzle
m	Mass of the gas molecule
m_{air}	Mass of the sample measured in the air
m_p	Mass flow rate of material (g/min)
m_{water}	Mass of the sample measured in distilled water
m_{gas}	Mass flow rate of gas (g/min)
M	Magnification factor of the image
M_t	Mass uptake of the sample at time (t); (g)
M_∞	Equilibrium mass uptake after an infinite time (g)
n	Degree of polymerization
n_1	Number of moles of solvent
n	Number of bubbles or cells
N_0 and N_1	Homogeneous and heterogenous bubble nucleation
N_0	Cell density (cells/cm ³)
P	Property of the bulk polymer
P_c	Critical pressure
P_f	Property of the foamed sample
P_i	Pressure inside the critical bubble
P_s	Pressure of the surrounding the bubble
P_{die}	Die pressure (Ps/s)

$P_{solubility}$	Solubility pressure of blowing agent (gas)
p	Characteristic of the material = $2100 \text{ N}\cdot\text{s}^{0.51}/\text{m}^2$
q	Characteristic of the material = 0.51
Q	Volume flow rate of the polymer/gas solution
r	Critical radius of the bubble
r_1 and r_2	Radius of bubble 1 and 2, respectively
R	Ideal gas constant (J/K)
R_{die}	Radius of the nozzle
$S(\theta)$	Function depending only on the wetting angle θ of the particle-gas interface
t	absorption time (s)
t_D	Time required for the completion of absorption (s)
t_s	Elapse time (s)
$t_{residence}$	Average residence time
T	Temperature in Kelvin (K)
T_c	Critical temperature ($^{\circ}\text{C}$)
T_c	Crystallization temperature ($^{\circ}\text{C}$)
T_g	Glass transition temperature ($^{\circ}\text{C}$)
T_m	Melting temperature or crystalline transition temperature ($^{\circ}\text{C}$)
v	Molar volume of the solvent
v_a	Expansion ratio of the sample
v_p	Specific volume of a material at room temperature
v_{gas}	Specific volume of blowing agent at the crystallization

V_f	Void fraction
x_1	Number of segment in the solvent molecule
z	Exponential equals 2 and 3/2 for the modulus and collapse stress
δ_1 and δ_2	Solubility parameters of solvent and polymer, respectively
ϕ_1 and ϕ_2	Volume fractions of solvent and polymer, respectively
ρ	Density of the un-foamed sample
ρ_f and ρ_{water}	Densities of the foamed sample and the water, respectively
χ	Flory-Huggins interaction parameter
η	Blowing agent efficiency
σ	Surface tension
ΔE_{mix}	Internal energy change upon isothermal evaporation of saturated liquid to the ideal gas state at infinite dilution
ΔG_{mix}	Total Gibb's free energy of mixing
ΔG_{homo}	Critical free energy to form a nucleus of critical size for homogeneous nucleation
ΔG_{het}	Critical free energy to form a nucleus of critical size for heterogeneous nucleation
ΔH_c	Enthalpy change of crystallization
ΔH_m	Enthalpy change of melting
ΔH_m^*	Enthalpy change of melting of the theoretical 100 % crystalline polymer
ΔS_{mix}	Entropy of mixing